Received: 21 December 2019 | Revised: 17 May 2020 | Accepted: 7 June 2020

DOI: 10.1002/humu.24062

RESEARCH ARTICLE

Human Mutation HGVS HUMAN GENOME VARIATION SOCIETY WILEY

First clinical and myopathological description of a myofibrillar myopathy with congenital onset and homozygous mutation in *FLNC*

Heike Kölbel[1] | Andreas Roos[1] | Peter F. M. van der Ven[2] | Teresinha Evangelista[3] | Kay Nolte[4] | Katherine Johnson[5] | Ana Töpf[5] | Michael Wilson[6,7] | Wolfram Kress[8] | Albert Sickmann[9,10,11] | Volker Straub[5] | Laxmikanth Kollipara[9] | Joachim Weis[4] | Dieter O. Fürst[2] | Ulrike Schara[1]

[1]Department of Pediatric Neurology, Developmental Neurology and Social Pediatrics, Children's Hospital University of Essen, Essen, Germany

[2]Department of Molecular Cell Biology, Institute for Cell Biology, University of Bonn, Bonn, Germany

[3]Neuromuscular Morphology Unit, Myology Institute, GHU Pitié-Salpêtrière, Paris, France

[4]Institute of Neuropathology, RWTH Aachen University Hospital, Aachen, Germany

[5]The John Walton Muscular Dystrophy Research Centre, Institute of Translational and Clinical Research, Newcastle University, Newcastle upon Tyne, UK

[6]Analytic and Translational Genetics Unit, Massachusetts General Hospital, Boston, Massachusetts

[7]Program in Medical and Population Genetics, Broad Institute of Harvard and MIT, Cambridge, Massachusetts

[8]Department of Human Genetics, University of Würzburg, Würzburg, Germany

[9]Department of Bioanalytics, Leibniz-Institut für Analytische Wissenschaften—ISAS—e.V., Dortmund, Germany

[10]Department of Chemistry, College of Physical Sciences, University of Aberdeen, Aberdeen, Scotland, UK

[11]Medizinische Proteom-Center (MPC), Medizinische Fakultät, Ruhr-Universität Bochum, Bochum, Germany

Correspondence
Heike Kölbel, Department of Pediatric Neurology, Developmental Neurology and Social Pediatrics, Children's Hospital University of Essen, Hufelandstraße 55, D-45147 Essen, Germany.
Email: heike.koelbel@uk-essen.de

Funding information
Muscular Dystrophy UK; Deutsche Forschungsgemeinschaft; Bundesministerium für Bildung und Forschung; AFM-Téléthon, Grant/Award Number: 21644; Samantha J Brazzo Foundation; LGMD2D Foundation and Kurt+Peter Foundation; European Regional Development Fund; Ultragenyx Pharmaceutical; Ministerium für Kultur und Wissenschaft des Landes Nordrhein-Westfalen; Limb Girdle Muscular Dystrophy 2i Research Fund; Regierende Bürgermeister von Berlin—inkl. Wissenschaft und Forschung; sanofi genzyme; Coalition to Cure Calpain-3

Abstract

Filamin C (encoded by the *FLNC* gene) is a large actin-cross-linking protein involved in shaping the actin cytoskeleton in response to signaling events both at the sarcolemma and at myofibrillar Z-discs of cross-striated muscle cells. Multiple mutations in *FLNC* are associated with myofibrillar myopathies of autosomal-dominant inheritance. Here, we describe for the first time a boy with congenital onset of generalized muscular hypotonia and muscular weakness, delayed motor development but no cardiac involvement associated with a homozygous *FLNC* mutation c.1325C>G (p.Pro442Arg). We performed ultramorphological, proteomic, and functional investigations as well as immunological studies of known marker proteins for dominant filaminopathies. We show that the mutant protein is expressed in similar quantities as the wild-type variant in control skeletal muscle fibers. The proteomic signature of quadriceps muscle is altered and ultrastructural perturbations are evident. Moreover, filaminopathy marker proteins are comparable both in our homozygous and a dominant control case (c.5161delG). Biochemical

investigations demonstrate that the recombinant mutant protein is less stable and more prone to degradation by proteolytic enzymes than the wild-type variant. The unusual congenital presentation of the disease clearly demonstrates that homozygosity for mutations in *FLNC* severely aggravates the phenotype.

KEYWORDS

congenital myopathy, filamin C, *FLNC*, myofibrillar myopathy, proteomic signature, recessive inheritance

1 | INTRODUCTION

Myofibrillar myopathies (MFMs) are a group of genetic muscle disorders characterized by histological abnormalities originating in the Z-disc, causing progressive disorganization of the intermyofibrillar network, build-up of abnormal protein inclusions, and vacuole formation within the sarcoplasm. MFM-causing genes encode a range of proteins related to the Z-disc, including *DES* (desmin), *CRYAB* (αB-crystallin), *MYOT* (myotilin), *FLNC* (filamin C), *ZASP* (LIM domain-binding protein 3), and *BAG3* (BAG family molecular chaperone regulator 3; Selcen, 2011). MFMs typically manifest in the third or fourth decade of life or later, although rare cases of adolescent onset have also been reported and show an autosomal-dominant inheritance pattern. Filamin C-related myopathies show three typical manifestations: (a) protein aggregation myopathy affecting skeletal and sometimes also cardiac muscles with initial proximal weakness caused by filamin C rod and dimerization domain mutations (Shatunov et al., 2009; Vorgerd et al., 2005), (b) distal myopathies due to haploinsufficiency or altered actin-binding capacity without protein aggregation pathology (Duff et al., 2011; Guergueltcheva et al., 2011), and (c) isolated cardiac phenotypes without symptoms of skeletal myopathy often caused by a premature stop codon in *FLNC* (Ader et al., 2019; Valdes-Mas et al., 2014). Patients with protein aggregation myopathy initially present with proximal muscle weakness, while distal and respiratory muscles become affected with disease progression (Furst et al., 2013).

Filamin C (FLNC) contains an N-terminal actin-binding domain (ABD) followed by a semiflexible rod domain comprising 24 immunoglobulin (Ig)-like folds that serve as an interface for interactions with numerous proteins (Furst et al., 2013; van der Flier & Sonnenberg, 2001). Notably, proteomic analysis of laser-microdissected protein aggregates from skeletal muscle fibers of MFM-filaminopathy patients allowed the identification of aggregate marker proteins including FLNC itself and many of its binding partners (Kley, Maerkens, et al., 2013). MFM-filaminopathy is associated with the expression of a toxic protein and not with reduced expression of FLNC. Here, for the first time, we describe a homozygous *FLNC* mutation leading to the manifestation of a severe myopathic phenotype. A combination of morphological, functional, and biochemical studies was performed to demonstrate pathogenicity. As the parents are asymptomatic and there is no family history of muscle disease, our data suggest that this novel c.1325C>G (p.Pro442Arg) mutation is the first recessive mutation to be described for *FLNC*.

2 | PATIENTS, MATERIALS, AND METHODS

2.1 | Patients

Muscle biopsies were obtained from the pediatric patient with the homozygous *FLNC* variant at the Department of Pediatric Neurology of Duisburg-Essen University as well as from one adult patient with a dominant mutation (c.5161delG) from the Institute of Myology in Paris.

Both biopsies were collected for diagnostic purposes, respectively. The biopsy derived from the adult case was used as a dominant disease control in our study. This adult patient (a 64-year-old male at the time of muscle biopsy, which has been performed in 2008) showed first symptoms around the age of 40 years with predominantly axial (unable to lift the head in supine position and to get out the bed without assistance) and proximal weakness more severe at the level of the lower limbs. Facial weakness was not noticed. Whereas distal upper limb muscles strength was normal, distal lower limb muscles showed weakness.

2.2 | Editorial policies and ethical considerations

Ethical approval was granted by the relevant local ethical committee of the participating centers of the MYO-SEQ project (14-6013-BO). Written informed consent was obtained from the legal guardians for the participation into the subsequent research and for publication of the findings.

2.3 | Genetic analysis

Exome sequencing and data analysis was performed as part of the MYO-SEQ project (Töpf et al., 2020). Sanger sequencing was performed in DNA to confirm the detected variants. Annotation of the *FLNC* gene is according to GenBank NC_000007.14 and transcript ENST00000325888. The c.1325C>G; p.Pro442Arg variant in *FLNC*, which we detected in our patient, is not observed in any current database of human genetic variations including the ExAC (http://exac.broadinstitute.org) and gnomAD (https://gnomad.broadinstitute.org) databases. In silico prediction modeling using different prediction tools lead to consistent variant classification of damaging (SIFT; https://sift.bii.a-star.edu.sg), possibly damaging (PolyPhen-2; http://genetics.bwh.harvard.edu/pph2) and disease-causing (MutationTaster; http://www.

mutationtaster.org), with a CADD score of 25, indicating that this change is among the top 0.3% most deleterious variants (https://cadd.gs.washington.edu).

2.4 | Histology and electron microscopy

Serial cryosections (10 μm) of transversely oriented muscle blocks were stained according to standard procedures with hematoxylin and eosin (H&E), Gömöri trichrome (GT), oil red O, adenosine triphosphatase (preincubation at pH 4.3 and 9.4), and nicotinamide adenine dinucleotide tetrazolium reductase (NADH-TR). Light microscopic investigations were performed using a Zeiss Axioplan epifluorescence microscope equipped with a Zeiss Axio Cam ICc 1. Glutaraldehyde-fixed muscle biopsy specimens from our patient were processed for ultrastructural examination by standard procedures. The tissue was postfixed in 1% osmium tetroxide and embedded in Epon 812. Semithin sections for light microscopy were stained with toluidine blue. Ultrathin sections were contrasted with uranyl acetate and lead citrate and examined using a Philips CM10 transmission electron microscope as described previously (Katona, Weis, & Hanisch, 2014).

2.5 | Proteomic profiling in human skeletal muscle

Analysis of the proteomic signature of the quadriceps muscle derived from the patient with the homozygous *FLNC* mutation was performed as described in Supporting Information Document S1.

2.6 | Immunological studies

Immunofluorescence studies were carried out on cryosections of our patient with the homozygous *FLNC* variant to study the distribution of FLNC and paradigmatic marker proteins of protein aggregates in filaminopathies (Kley, Maerkens, et al., 2013), to verify the proteomic findings and to compare them with those from a patient with a heterozygous dominant *FLNC* mutation (Rossi et al., 2017). Applied techniques were described previously (Kley, van der Ven, et al., 2013; Kolbel et al., 2019; Roos et al., 2014). Antibodies used for this purpose are listed in Supporting Information Document S1. Light microscopic investigations were performed using a Zeiss Axioplan epifluorescence microscope equipped with a Zeiss Axio Cam ICc 1.

Immunoblot analyses were carried out as described previously (Roos et al., 2014) utilizing the same FLNC antibody (1:500) as for the immunofluorescence studies (see above).

2.7 | In vitro analysis of stability of mutant versus wild-type FLNC

To investigate the susceptibility of mutant and wild-type FLNC to proteolytic digestion, recombinantly expressed wild-type and mutant FLNC fragments encompassing Ig domains one to three (d1–3) were incubated with the endopeptidase thermolysin under native conditions. Hence, 3 μl of 100 μg/ml thermolysin solution (Sigma-Aldrich) was added to 20 μg purified protein solubilized in 140 μl 50 mM NaH_2PO_4, 300 mM NaCl, 250 mM imidazole, pH 8.0, and the mixture was incubated at 37°C. After different incubation times, the reaction was stopped by addition of 0.2 volumes of 5× SDS (sodium dodecyl sulfate) sample buffer. Samples were heated for 5 min at 95°C and analyzed by sodium dodecyl sulfate polyacrylamide gel electrophoresis (SDS-PAGE).

3 | RESULTS

3.1 | Clinical presentation

The patient is the first child of non-consanguineous parents. After an uneventful pregnancy and normal birth, the mother recognized weak sucking in the first month of life. An inguinal hernia operation was performed at the age of 3 months. Due to motor development delay, the patient was unable to pivot. Moreover, generalized muscular hypotonia with frog-leg posture and contractures in both knees were noticed. Physiotherapy was started and at 10 months of age the boy achieved free sitting after being placed. At the age of 14 months he began to crawl. At the same age, neuropediatric consultation revealed general muscular hypotonia and weakness, a pectus carinatum, a gothic palate, chewing difficulties, and no reflexes. Motor neurography showed normal amplitudes of the muscle action potential and normal conduction velocities. All sensory and F-wave conduction velocities were normal, thereby excluding a general neuropathy or significant α-motoneuron decay. The serum creatine kinase level was not elevated and examination of *SMN1* gene revealed no mutations. Based on the proximal weakness the child achieved the ability of free walking at the age of 28 months. After febrile infections a worsening of the symptoms were notable. Up to now, several examinations excluded cardiac involvement. However, the boy was examined twice a year with pulmonary function test and developed a restrictive ventilatory problem (FVC 61%) and a reduced peak cough flow (140 L/min) with no acute need for noninvasive or invasive ventilation. At the age of 10 years, he could independently walk 200 m, but needed assistance when climbing stairs. He showed normal speech and cognitive development. At his last visit at the age of 13 years, he had lost ambulation. Progressive loss of proximal and (later) distal muscle mass is illustrated in Figure 1a. A myopathic face or weak neck flexors were not noticed in the progression of the disease.

The parents (aged 42 and 49 years, respectively) are clinically examined and unaffected, so far. Furthermore, three subsequent generations of the family revealed no prevalence of a neuromuscular or cardiac disease.

3.2 | Molecular genetic findings

Exome sequencing was carried out on DNA extracted from blood in the framework of the MYO-SEQ project (Töpf et al., 2020) by

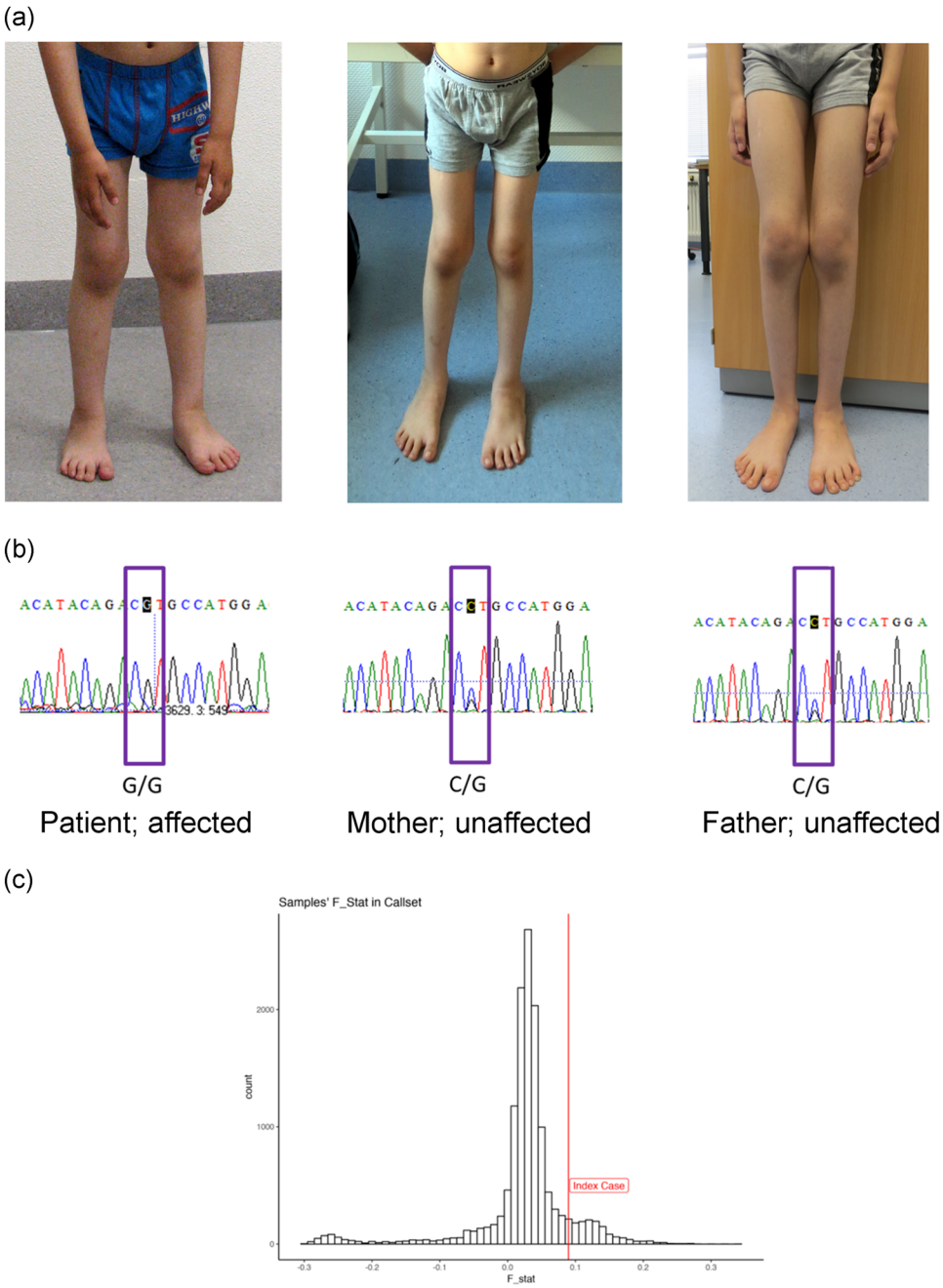

FIGURE 1 Clinical and molecular genetic findings. (a) Progressive muscle wasting: left—knee contractures and muscular hypotonia at the age of 2 years; middle—mild proximal involvement at the age of 5 years; right—distal myopathy combined with proximal involvement at the age of 10 years. (b) Sanger sequencing electropherograms showing a homozygous c.1325C>G nucleotide substitution in the index patient while both parents are heterozygous for the mutation. (c) The figure displays computed method-of-moments *F* coefficient estimates for all samples in a callset. The coefficients were generated using PLINK's-het method over 88,393 SNPs for each sample to calculate (observed autosomal homozygous genotype count − expected count)/(total observations − expected count) where the expected counts are based on imputed MAFs. MAFs, minor allele frequencies; SNPs, single-nucleotide polymorphisms

focusing on potential mutations in a list of selected 169 genes that are known to be associated with manifestation of neuromuscular disorders (list is available on request). This analysis revealed a homozygous mutation in exon 8 of the *FLNC* gene (hg19: chr7:128478771C>G; c.1325C>G; p.Pro442Arg) that would lead to exclusive expression of FLNC with a p.Pro442Arg substitution in Ig-like domain 2 of the FLNC rod domain. This variant is absent in Exac, gnomAD, and 1,000 genomes. Homozygosity of the mutation was confirmed by Sanger sequencing. The mutation was found in a heterozygous status in the thus far clinically unaffected parents (Figure 1b). No other homozygous variants with Variant Effect Predictor (VEP) mod to high and minor allele frequency (MAF) < 0.01

were found in any of the analyzed genes. Computed method-of-moments *F* coefficient estimates for all samples in a callset estimated a value for this family of 0.089. Given that this value is higher than it would be expected (>0.05) one might conclude that even if the parents are not knowingly consanguineous it would appear that they are related (Figure 1c).

3.3 | Histological findings

Quadriceps muscle biopsy taken at the age of 30 months, showed mild variation in fiber size, atrophied fibers, and amorphous eosinophilic deposits on H&E stain (Figure 2a, a1, a2). ATPase treatment (pH 9.4) demonstrated fiber-type I predominance (Figure 2a, a3). Moreover, modified GT staining revealed subsarcolemmal enrichment of amorphous material and sharply circumscribed areas with decreased enzyme activity in many abnormal fiber regions (Figure 2a, a4). Nicotinamide adenine dinucleotide (NADH) muscle histology revealed increased enzyme activity in subsarcolemmal areas (black arrows in Figure 2a, a5–a7), weak myofibrillar NADH-TR activity, and core-like fibers with unstained central areas (white arrows in Figure 2a, a5, a6) as well as whorls (Figure 2a, a7). Increased enzyme activity in subsarcolemmal areas (black arrows in Figure 2a, a8) and weak myofibrillar enzyme activity with central unstained areas was observed in COX (cytochrome *c* oxidase)-/SDH (succinate dehydrogenase)-stained muscle sections (see white arrows in Figure 2a, a8). Periodic acid–Schiff (PAS) staining also revealed sarcoplasmic areas with reduced labeling (white arrows in Figure 2a, a9) as well as increased labeling of vacuoles (black arrows in Figure 2a, a9).

3.4 | Electron microscopic findings

Ultrastructural findings comprised ring fibers and subsarcolemmal depositions including elements of degenerated myofibrils and other sarcoplasmic components. In addition, muscle fibers with grouped electron-dense inclusions reminiscent of myofibrillar rods, probably representing advanced sarcomeric lesions, were observed (Figure 2b).

3.5 | Proteomic findings

Proteomics is a powerful tool for the unbiased investigation of pathophysiological processes in rare disorders such as neurodegenerative and neuromuscular diseases (Roos, Thompson, Horvath, Lochmuller, & Sickmann, 2018). Here, we studied the proteomic signature of the patient-derived quadriceps using quantitative mass spectrometry. We identified 33 differentially abundant proteins associated with the expression of c.1325C>G/p.Pro442Arg mutant *FLNC*/FLNC; of these 29 were upregulated and 4 downregulated (Figure 3a). A proteomaps-based pathway analysis (www.proteomaps.net) revealed that altered protein abundances, apart from cytoskeleton, also impinge on alterations in cellular mechanisms such as signaling pathways and complement activation (Figure 3b). Moreover, functional information of the affected proteins from uniprot (www.uniprot.org) showed that proteins involved in muscle regeneration are increased along with alpha-1-antichymotrypsin, which is a biomarker of muscle atrophy (Table 1). An analysis of functional protein association networks via STRING (www.string-db.org) revealed a functional interplay of a proportion of proteins affected by the homozygous expression of mutant FLNC in the muscle fibers of our patient carrying the homozygous variant (Figure 3c). Notably, altered abundances of some of these proteins can be linked to known FLNC functions and might suggest activation of compensatory mechanisms: galectin-3, increased in patient-derived quadriceps muscle, is known to promote myogenesis and increase transketolase as a modulator of sugar metabolism might counteract loss of FLNC function in metabolic processes (see below).

3.6 | Immunological findings

Immunofluorescence examinations performed in the context of a routine diagnostic work-up showed reduced expression of dystrophin 2, dystrophin 3, and alpha-dystroglycan (data not shown), while muscle fibers showed focally increased abundance of desmin, alpha-actinin, myotilin, and FLNC (Figure 4a, a1–a4) in the sarcoplasmic and subsarcolemmal mass. The immunoblot analysis showed no reduction of the FLNC amount (Figure 5b). Laser-capture microdissection and subsequent mass spectrometric analysis of protein aggregates derived from skeletal muscle fibers of MFM-filaminopathy patients allowed the definition of a set of marker proteins for protein aggregate formation in this subtype of structural myopathies (Kley, Maerkens, et al., 2013). To investigate pathogenicity of the c.1325C>G (p.Pro442Arg) variant, a total of eight marker proteins were analyzed. Four of these markers (myomesin, myopodin, Xin, and XIRP2) are defined markers for MFMs including filaminopathies (Claeys et al., 2009). The other four (vimentin, lamin A/C, Rab35, and dysferlin) were identified by proteomic investigation of protein aggregates of filaminopathy patients (Kley, Maerkens, et al., 2013). Examinations of protein distribution were based on immunofluorescence and/or immunohistochemistry studies utilizing muscle biopsy sections derived from our patient and a case with a described dominant form of filaminopathy (as disease control; see above) as well as two age-matched control muscles. Co-immunofluorescence-based studies of the distribution of myomesin, myopodin, Xin, and XIRP2 revealed FLNC aggregates, which also presented immunoreactivity Xin and XIRP2, and to a weaker degree with myopodin and myomesin (Figure 4). Moreover, our studies revealed occasionally small Rab35-immunoreactive deposits, which are more frequent in the quadriceps muscle of the c.1325C>G (p.Pro442Arg) patient (white arrows in Figure 4c). Immunolocalization of dysferlin revealed a conspicuous accumulation of the protein in subsarcolemmal regions (white arrows in Figure 4c) in our patient that

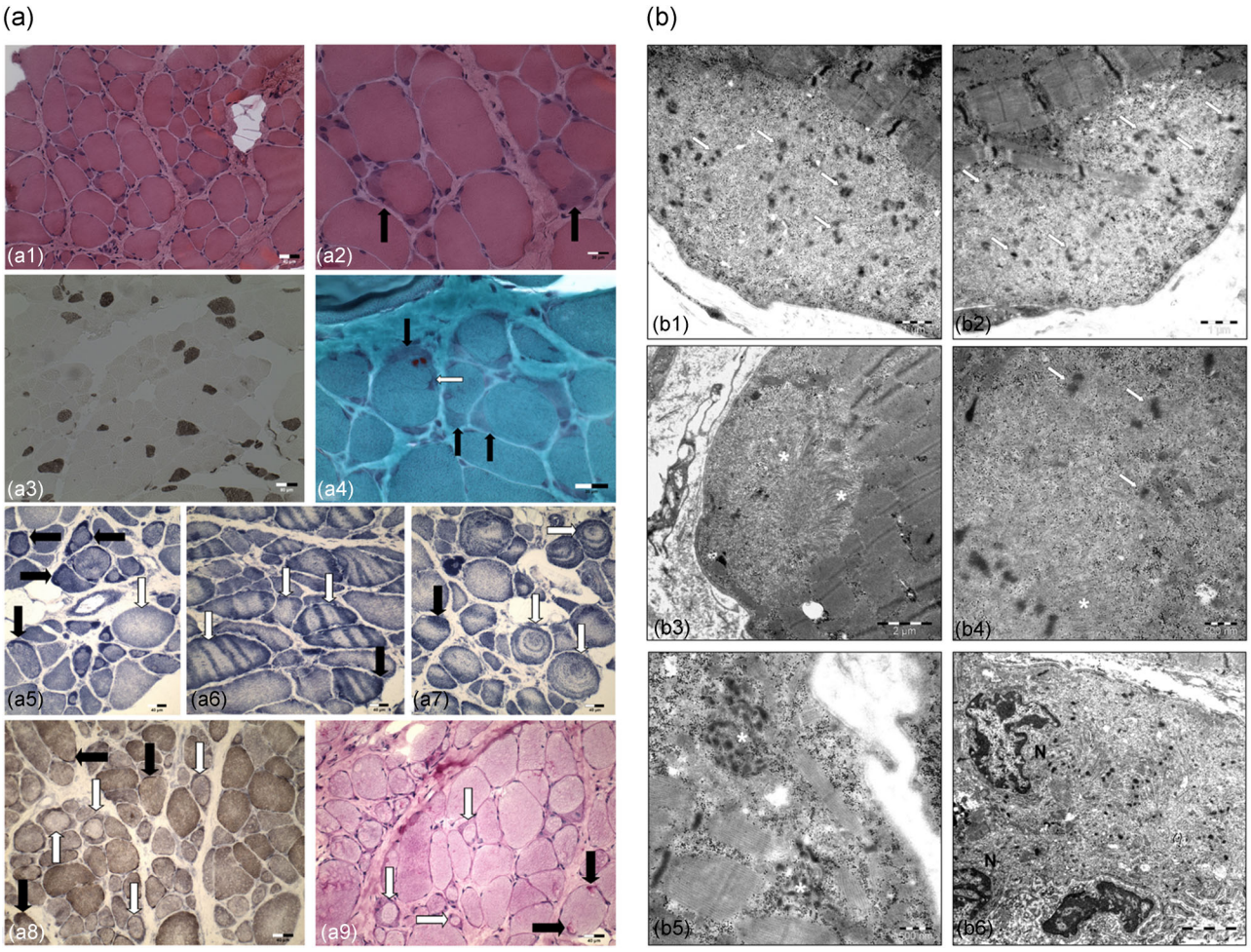

FIGURE 2 (a) Muscle histology and enzyme histochemistry in c.1325C>G/p.Pro442Arg *FLNC*/FLNC mutant quadriceps muscle. (a1 and a2) H&E staining revealed mild variation in fiber size, atrophied fibers, and subsarcolemmal amorphous eosinophilic deposits (black arrows). (a3) ATPase treatment (pH 9.4) revealed fiber-type I predominance. (a4) Modified Gömöri trichrome-stained muscle fibers show subsarcolemmal enrichment of amorphous material (black arrows), sharply circumscribed decrease of enzyme activity and sarcoplasmic enrichment of amorphous material (white arrow). (a5–a7) NADH muscle histology revealed subsarcolemmal increased enzyme activity (black arrows), weak myofibrillar NADH-TR activity, core-like fibers with central unstained areas, and whorls (white arrows). (a8) COX/SDH-stained muscle fibers show increased enzyme activity in subsarcolemmal areas (black arrows) and weak myofibrillar enzyme activity with central unstained areas (white arrows). (a9) PAS staining revealed sarcoplasmic areas of reduced labeling (white arrows) as well as increased labeling in vacuoles (black arrows). (b) Occasionally ring fibers are seen (asterisks: misoriented myofibrills) displaying subsarcolemmal areas of advanced myofibrillar dissolution. Here, clumped filaments resembling Z-disc material (arrows) are a frequent finding (b1, bar = 1 μm). Ring fiber with disorientated myofibrils (asterisks) ending up in subsarcolemmal deposits including glycogen, elements of degenerated myofibrils (Z-disc remnants, arrows), and other sarcoplasmic components (b2, bar = 1 μm). Subsarcolemmal accumulation of myofibrillar debris including filamentous material (asterisks) (b3, bar = 2 μm). Cytoplasmic zone of myofibrillolysis and abnormal deposition of glycogen and Z-disc-associated proteins (arrows) as well as granulofilamentous material (asterisk) (b4, bar = 500 nm). Muscle fiber with grouped electron-dense (lipo-)protein aggregates (asterisks) (b5, bar = 500 nm). Large subsarcolemmal deposits also occur without adjacent misorientated myofibrils. Note hyperlobulated myonuclei (N) (b6, bar = 2 μm). COX/SDH, cytochrome *c* oxidase/succinate dehydrogenase; H&E, hematoxylin and eosin; NADH, nicotinamide adenine dinucleotide; NADH-TR, nicotinamide adenine dinucleotide tetrazolium reductase; PAS, periodic acid–Schiff

was accompanied by a reduced staining of the sarcolemmal region in other areas. In the muscle fibers of the heterozygous patient, only few dysferlin-immunoreactive irregular sarcoplasmic dots were observed (white arrows in Figure 4c).

Moreover, we observed subsarcolemmal deposits immunoreactive for vimentin in both patients, which were more frequently present in the sarcoplasm in the muscle biopsy of the dominant case (white arrows in Figure 4c).

Immunohistochemistry studies of lamin A/C revealed in both cases sarcoplasmic deposits immunoreactive for lamin A/C (white arrows in Figure 4c), which might result from nucleophagy of centralized myonuclei. These deposits were more pronounced in the case carrying the dominant *FLNC* mutation.

Given that our proteomic profiling approach focused on potential changes of protein signature in the entire muscle upon expression of mutant FLNC, we next confirmed the altered

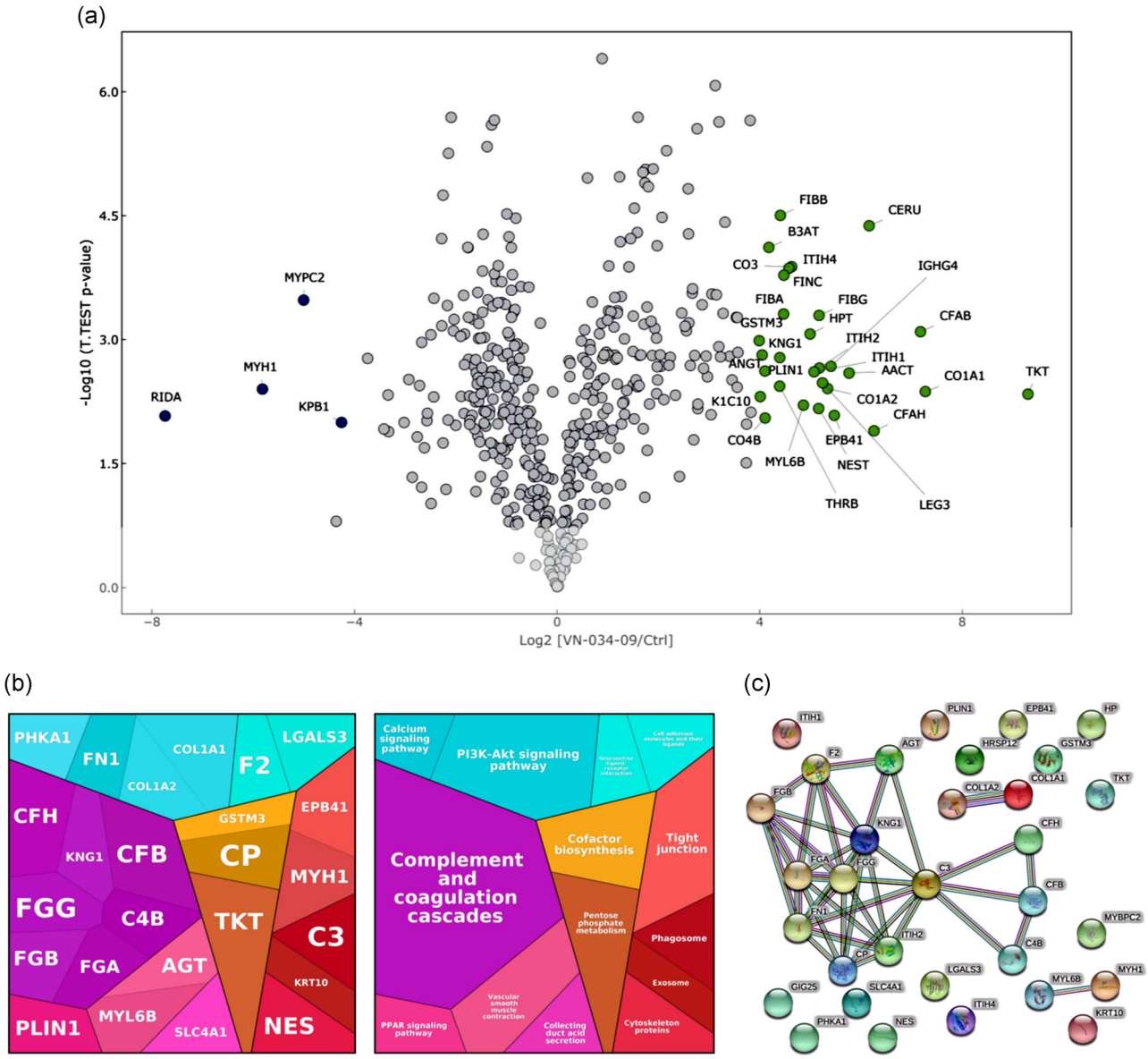

FIGURE 3 Proteomic profiling and subsequent data analysis. (a) Volcano-plot (Nolte, MacVicar, Tellkamp, & Krüger, 2018) of proteomic findings showing reduced abundance of 4 (blue dots) and increased abundance of 29 proteins (green dots) indicating pathogenicity of c.1325C>G/p.Pro442Arg mutant *FLNC*/FLNC. (b) Proteomaps-based pathway analysis revealed that altered protein abundances affect cytoskeleton and further cellular mechanisms including signaling pathways and complement activation. (c) STRING-protein network analysis (highest confidence 0.9 interaction evidence setting) revealed a functional interplay of a proportion of proteins affected by the homozygous expression of mutant FLNC in the muscle

abundances of galectin-3 and transketolase. Hereby, galectin-3 was selected as it is known to promote myogenesis (Rancourt et al., 2018) and transketolase (involved in sugar metabolism) based on the fact that FLNC is known to be involved in regulation of metabolic processes (Furst et al., 2013; Leber et al., 2016; Molt et al., 2014). These studies revealed a (sub)sarcolemmal increase of galectin-3 in both, the recessive and the dominant case (white arrows in Figure 4c). Moreover, in both cases, sarcoplasmic deposits immunoreactive for galectin-3 were identified (white arrows in Figure 4c). For transketolase, a cellular increase could be observed in both, the recessive and the dominant case whereby the elevation seemed to be more pronounced in the dominant case (white arrows in Figure 4c).

3.7 | In vitro versus ex vivo analysis of stability of mutant versus wild-type FLNC

Improperly folded and unstable proteins are often more prone to degradation by proteolytic enzymes. The fact that it was more difficult to obtain sufficient amounts of purified mutant protein may already be taken as an indication for reduced stability. To prove this

TABLE 1 Detailed information on proteins showing affected abundance associated with the homozygous expression c.1325C>G (p.Pro442Arg) of mutant FLNC

	Unique peptides	Protein	Gene	Ratio (Pat./Ctrl.)	Log2 (Pat./Ctrl.)	*t* test	Function	Associated disease
P29401	2	Transketolase	*TKT*	629.35	9.30	0.00	Catalyzes the transfer of a two-carbon ketol group from a ketose donor to an aldose acceptor	OMIM: 617044; short stature, developmental delay, and congenital heart defects (SDDHD)
P02452	7	Collagen alpha-1	*CO1A1*	154.38	7.27	0.00	Member of group I collagen (fibrillar-forming collagen)	OMIM: 114000; Caffey disease (CAFFD)
P00751	6	Complement factor B	*CFAB*	144.59	7.18	0.00	Factor B, which is part of the alternate pathway of the complement system	OMIM: 615489; macular degeneration, age-related, 14 (ARMD14)
P08603	2	Complement factor H	*CFAH*	76.57	6.26	0.01	Accelerates the decay of the complement alternative pathway (AP) C3 convertase C3bBb, thus preventing local formation of more C3b	OMIM: 609814; complement factor H deficiency (CFHD)
P00450	5	Ceruloplasmin	*CERU*	71.60	6.16	0.00	Involved in iron transport across the cell membrane; plays a role in fetal lung development or pulmonary antioxidant defense	OMIM: 604290; cerebellar ataxia
P01011	4	Alpha-1-antichymotrypsin	*SERPINA3*	54.40	5.77	0.00	Inhibitor of neutrophil cathepsin G	Represents a circulating biomarker of muscle atrophy associated to glucocorticoid and, broadly, a reflection of dynamic changes in muscle mass (Gueugneau et al., 2018)
P11171	2	Protein 4.1	*EPB41*	44.41	5.47	0.01	Regulating membrane physical properties of mechanical stability and deformability by stabilizing spectrin–actin interaction as well as binds and regulates myosin (Pasternack & Racusen, 1989)	OMIM: 611804; elliptocytosis 1 (EL1)
P01861	3	Immunoglobulin heavy constant gamma 4	*IGHG4*	42.42	5.41	0.00	Constant region of immunoglobulin heavy chains	
P08123	3	Collagen alpha-2	*CO1A2*	40.56	5.34	0.00	Member of group I collagen (fibrillar-forming collagen)	OMIM: 617821; Ehlers-Danlos syndrome, arthrochalasia type, 2 (EDSARTH2)
P17931	2	Galectin-3	*LEG3*	37.82	5.24	0.00	Coordinates the recognition of membrane damage with mobilization of the core autophagy regulators ATG16L1 and BECN1 in response to damaged endomembranes	Promotes myogenesis and improves skeletal muscle function in the mdx model of Duchenne muscular dystrophy (DMD; Rancourt et al., 2018)
P19823	4	Inter-alpha-trypsin inhibitor heavy chain H2	*ITIH2*	36.21	5.18	0.00	Regulates the localization, synthesis, and degradation of hyaluronan	

(Continues)

TABLE 1 (Continued)

	Unique peptides	Protein	Gene	Ratio (Pat./Ctrl.)	Log2 (Pat./Ctrl.)	*t* test	Function	Associated disease
P02679	6	Fibrinogen gamma chain	*FIBG*	36.08	5.17	0.00	Polymerizes to form an insoluble fibrin matrix; facilitates the antibacterial immune response via both innate and T-cell-mediated pathways	OMIM: 202400; congenital afibrinogenemia (CAFBN)
P48681	3	Nestin	*NEST*	35.87	5.16	0.01	Promotes the disassembly of phosphorylated vimentin intermediate filaments (IFs); contributes to skeletal muscle homeostasis and regeneration (Lindqvist et al., 2017)	
P19827	2	Inter-alpha-trypsin inhibitor heavy chain H1	*ITIH1*	33.68	5.07	0.00	Regulates the localization, synthesis, and degradation of hyaluronan	
P00738	6	Haptoglobin	*HPT*	31.90	5.00	0.00	Acts as an antioxidant, has antibacterial activity, and plays a role in modulating many aspects of the acute phase response	OMIM: 614081; anhaptoglobinemia (AHP)
P14649	11	Myosin light chain 6B	*MYL6B*	29.13	4.86	0.01	Regulatory light chain of myosin	
P01024	21	Complement C3	*CO3*	24.78	4.63	0.00	Plays a central role in the activation of the complement system; facilitates skeletal muscle regeneration by regulating monocyte function and trafficking (Zhang et al., 2017)	OMIM: 613779; complement component 3 deficiency (C3D)
P02751	2	Fibronectin	*FINC*	23.91	4.58	0.00	Induces fibril formation; impacts on the regenerative capacity of murine skeletal muscle (Lukjanenko et al., 2016)	
Q14624	2	Inter-alpha-trypsin inhibitor heavy chain H4	*ITIH4*	22.28	4.48	0.00	Involved in inflammatory responses to trauma	
P02671	4	Fibrinogen alpha chain	*FIBA*	22.22	4.47	0.00	Pro-inflammatory effect of fibrinogen on vascular smooth muscle cells by regulating the expression of PPARα, PPARγ, and MMP-9 (Wang et al., 2015)	OMIM: 202400; congenital afibrinogenemia (CAFBN)
P02675	9	Fibrinogen beta chain	*FIBB*	21.25	4.41	0.00		
P01042	3	Kininogen-1	*KNG1*	21.08	4.40	0.00	Inhibitor of thiol proteases	Predictive biomarker for the response of patients with dilated cardiomyopathy to immunoadsorption therapy (Bhardwaj et al., 2017)

TABLE 1 (Continued)

	Unique peptides	Protein	Gene	Ratio (Pat./Ctrl.)	Log2 (Pat./Ctrl.)	*t* test	Function	Associated disease
P00734	2	Prothrombin	*THRB*	21.04	4.40	0.00	Converts fibrinogen to fibrin and activates factors V, VII, VIII, XIII, and, in complex with thrombomodulin, protein C; also functions in inflammation	
P02730	6	Band 3 anion transport protein	*B3AT*	18.15	4.18	0.00	Functions both as a transporter that mediates electroneutral anion exchange across the cell membrane and as a structural protein	OMIM: 612653; spherocytosis 4 (SPH4)
P0C0L5	9	Complement C4-B	*CO4B*	17.24	4.11	0.01	Catalyzes the transacylation of the thioester carbonyl group to form ester bonds with carbohydrate antigens	
O60240	4	Perilipin-1	*PLIN1*	17.19	4.10	0.00	Coats lipid storage droplets to protect them from breakdown	OMIM: 613877; lipodystrophy, familial partial, 4 (FPLD4)
P01019	3	Angiotensinogen	*ANGT*	16.55	4.05	0.00	Essential component of the renin–angiotensin system	Involved in the development of insulin resistance associated with postinfarct heart failure in mice (Fukushima et al., 2014)
P13645	5	Keratin, type I cytoskeletal 10	*K1C10*	16.13	4.01	0.00	Plays a role in the establishment of the epidermal barrier on plantar skin	OMIM: 113800; epidermolytic hyperkeratosis (EHK)
P21266	2	Glutathione S-transferase Mu 3	*GSTM3*	15.90	3.99	0.00	Conjugation of reduced glutathione to a wide number of exogenous and endogenous hydrophobic electrophiles	
P46020	2	Phosphorylase b kinase regulatory subunit alpha, skeletal muscle isoform	*KPB1*	0.05	−4.26	0.01	Phosphorylase b kinase catalyzes the phosphorylation of serine in certain substrates, including troponin I	OMIM: 300559; glycogen storage disease 9D (GSD9D)
Q14324	25	Myosin-binding protein C, fast-type	*MYPC2*	0.03	−5.00	0.00	Binds MHC, F-actin and native thin filaments, and modifies the activity of actin-activated myosin ATPase. It may modulate muscle contraction or may play a more structural role	
P12882	17	Myosin-1	*MYH1*	0.02	−5.82	0.00	Muscle contraction	
P52758	2	2-iminobutanoate/2-iminopropanoate deaminase	*RIDA*	0.00	−7.74	0.01	Catalyzes the hydrolytic deamination of enamine/imine intermediates that form during the course of normal metabolism	

Abbreviations: Ctrl., control; OMIM, Online Mendelian Inheritance in Man; Pat., patient.

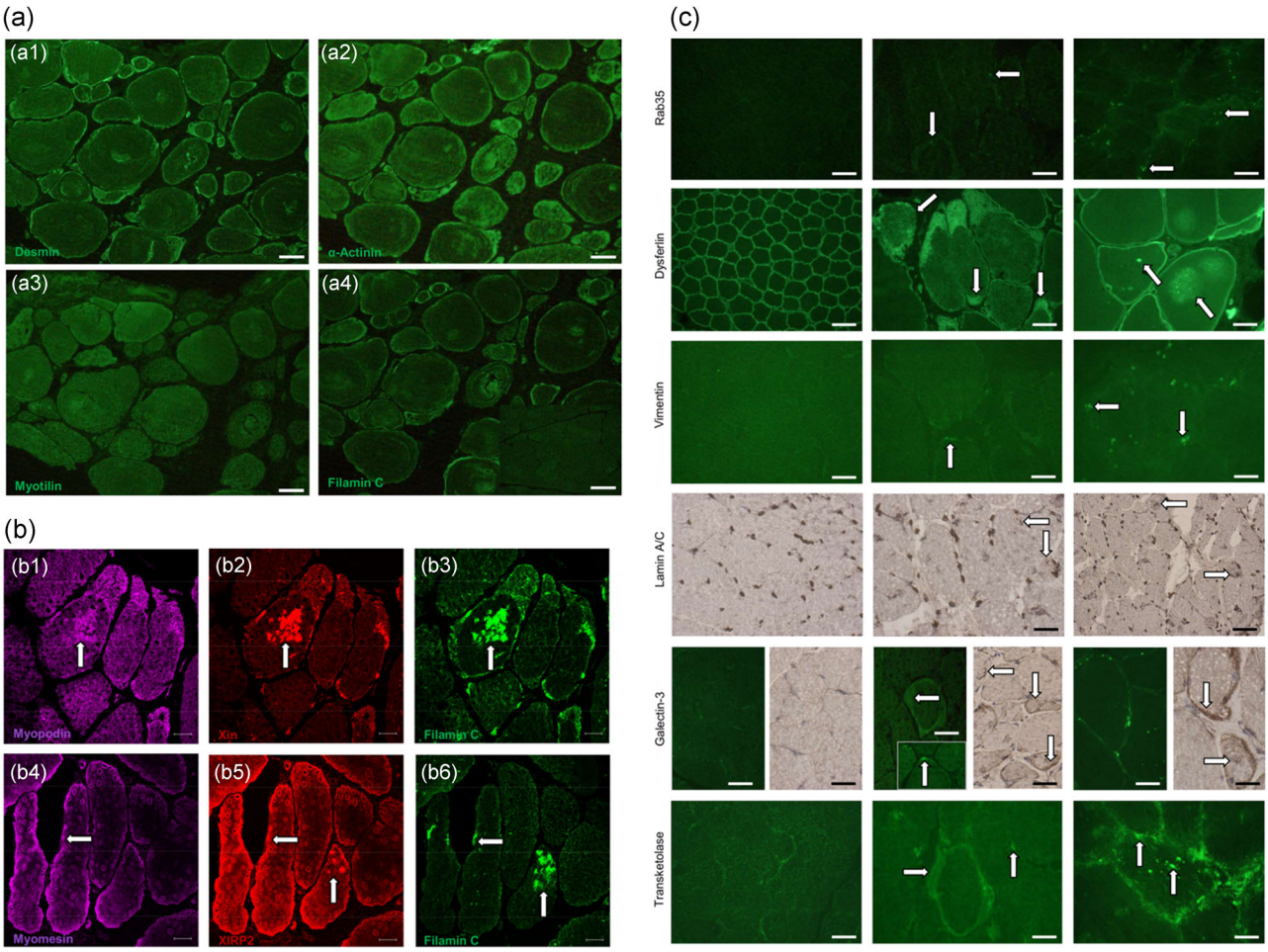

FIGURE 4 Immunological studies of filaminopathy marker proteins. (a) Immunofluorescence-based investigation of structural proteins including desmin, alpha-actinin, myotilin, and FLNC revealed irregular localizations along with increased immunoreactivity. (b) Co-immunofluorescence-based studies of FLNC, myopodin, myomesin, XIRP2, and Xin revealed the presence of FLNC aggregates also immunoreactive for myopodin and Xin (b1–b3) as well as also for XIRP and occasionally myomesin (b4–b6). (c) Analysis of expression and distribution of filaminopathy protein aggregate markers Rab35, dysferlin, vimentin, and lamin A/C showed focal sarcoplasmic and sarcolemmal increase (white arrows) compared with investigated controls (one representative control is shown/left column). The pathological protein distributions were usually more pronounced in the quadriceps muscle biopsy derived from the patient carrying the dominant *FLNC* mutation. Antibody-based immunofluorescence labeling of galectin-3 and transketolase also revealed focal sarcoplasmic and sarcolemmal increase of the proteins in the muscle biopsies derived from the filaminopathy patients with a more pronounced effect in the dominant case (white arrows) compared to the investigated controls (one representative control is shown)

assumption, corresponding wild-type and mutant protein fragments comprising domains 1–3 were treated with the protease thermolysin, an enzyme that preferentially cleaves proteins before leucine and phenylalanine residues. In this assay, natively folded proteins are a lot more stable than proteins, which have problems acquiring or stabilizing their tertiary structure. Gel-electrophoretic analysis of the resulting digests revealed that, in contrast to the wild-type variant, the mutant protein was already partially digested after 5 min of incubation, with the largest part digested after an incubation time of 40 min, while the wild-type protein was essentially not digested (Figure 5a). This indicates that the c.1325C>G (p.Pro442Arg) mutation causes misfolding of FLNC resulting in increased susceptibility to proteolysis in solution. Proteomic profiling revealed no significant differences in the expression level of FLNC between control muscles and the patient-derived muscle sample as exemplified by the 3D-montages for the peptide APLQVAVLGPTGVAEPVEVR (Figure 5c). Ratios for further peptides unique for FLNC confirmed highly similar protein levels (Figure 5d). This indicates that high levels of misfolded FLNC protein are expressed in the muscle fibers of our homozygous c.1325C>G (p.Pro442Arg) patient.

To summarize our combined proteomic and immunological findings, unbiased analyses of the protein signature of homozygous c.1325C>G/p.Pro442Arg *FLNC*/FLNC mutant quadriceps muscle allowed the identification of novel marker proteins (of pathophysiological relevance), which could be confirmed in an additional biopsy derived from patient suffering from a dominant *FLNC* mutation. Moreover, known marker proteins for dominant filaminopathies could be confirmed in our case. These combined findings support the

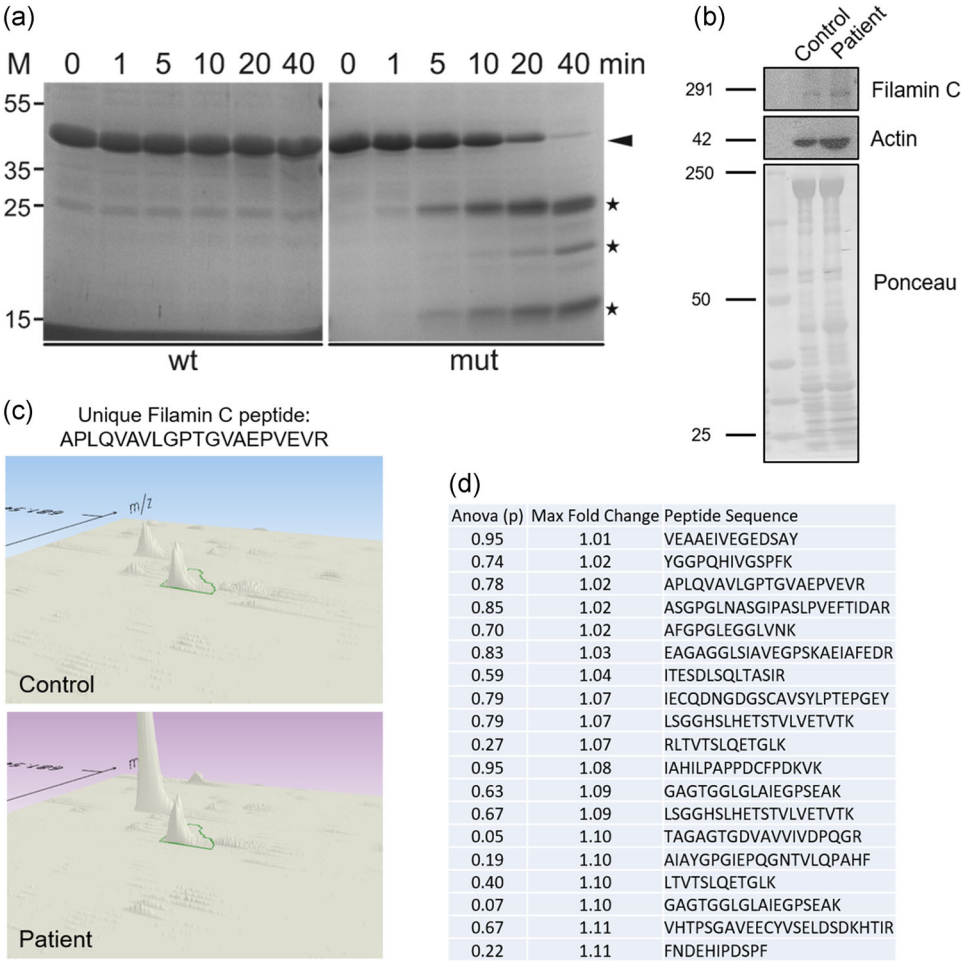

Anova (p)	Max Fold Change	Peptide Sequence
0.95	1.01	VEAAEIVEGEDSAY
0.74	1.02	YGGPQHIVGSPFK
0.78	1.02	APLQVAVLGPTGVAEPVEVR
0.85	1.02	ASGPGLNASGIPASLPVEFTIDAR
0.70	1.02	AFGPGLEGGLVNK
0.83	1.03	EAGAGGLSIAVEGPSKAEIAFEDR
0.59	1.04	ITESDLSQLTASIR
0.79	1.07	IECQDNGDGSCAVSYLPTEPGEY
0.79	1.07	LSGGHSLHETSTVLVETVTK
0.27	1.07	RLTVTSLQETGLK
0.95	1.08	IAHILPAPPDCFPDKVK
0.63	1.09	GAGTGGLGLAIEGPSEAK
0.67	1.09	LSGGHSLHETSTVLVETVTK
0.05	1.10	TAGAGTGDVAVVIVDPQGR
0.19	1.10	AIAYGPGIEPQGNTVLQPAHF
0.40	1.10	LTVTSLQETGLK
0.07	1.10	GAGTGGLGLAIEGPSEAK
0.67	1.11	VHTPSGAVEECYVSELDSDKHTIR
0.22	1.11	FNDEHIPDSPF

FIGURE 5 Analysis of FLNC stability. (a) Investigation via thermolysin digestion: wild-type (wt) and c.1325C>G/p.Pro442Arg mutant (mut) *FLNC*/FLNC d1–3 fragments were treated with the protease thermolysin for 1–40 min, as indicated above each lane. Samples were analyzed by polyacrylamide gel electrophoresis. Note that the mutant protein was already partly digested after an incubation time of 5 min, and almost completely digested after 40 min, while the wild-type variant was still completely intact after 40 min of incubation, indicating less stable folding of the mutant protein. Black arrowhead: intact FLNc d1–3. Stars: proteolyzed protein fragments. (b) Western blot analysis of FLNC abundance: Investigation of FLNC and actin revealed no reduction in the level of these two structural proteins compared to the level detected in whole muscle protein extract derived from a control individual. Ponceau red staining of the PVDF membrane was used to visualize concentration of whole protein loading. (c) 3D-montage (Progenesis) of the unique tryptic FLNC peptide APLQVAVLGPTGVAEPVEVR showing similar abundances in whole quadriceps muscle protein extracts of a control and the patient carrying the c.1325C>G (p.Pro442Arg) mutation. (d) Listing of ratios of abundances of unique tryptic peptides for FLNC in whole protein extracts of control and patient-derived muscle revealing no significant changes based on the presence of the c.1325C>G (p.Pro442Arg) mutation. PVDF, polyvinylidene difluoride

concept of the homozygous c.1325C>G/p.Pro442Arg *FLNC*/FLNC mutation being causative for the manifestation of a filaminopathy characterized by the expression of a mutant protein with presumably altered stability.

4 | DISCUSSION

We have for the first time identified a homozygous missense mutation in the *FLNC* gene in our pediatric patient that results in an amino acid exchange of proline to arginine. This mutation was not found in several genetic databases and control populations (dbSNP, ESP, ExAC, and gnomAD) or as a causal mutation in the literature. Algorithms to predict the deleteriousness of this amino acid exchange classify this variant as probably pathogenic, and within the 0.3% most damaging variants of the genome. Mechanical instability of mutant FLNC and associated reduced strain resistance of myofibrillar Z-discs are well-known major pathophysiological cascades in MFM-filaminopathy, first identified in the most prevalent human *FLNC* mutation p.2710X and the corresponding heterozygous mouse knock-in model (Chevessier et al., 2015). The impaired protein stability is the basis of the formation of micro- and macro-lesions, which were suggested to be preclinical disease stages preceding the development of the characteristic protein aggregates (Chevessier et al., 2015). Our proteomic findings and Western blot analysis experiments revealed no changes in the expression level of FLNC

between the pediatric patient and respective control muscle protein extract, indicating that the observed phenotype is not a consequence of reduced amounts of FLNC. Instead, our in vitro protein stability studies revealed that the c.1325C>G/p.Pro442Arg mutant *FLNC*/FLNC revealed that the mutant protein is clearly more susceptible to proteolysis by the protease thermolysin, probably due to misfolding of Ig-like domain 2. Within *FLNC* the proline residue at amino acid position 422 is conserved across all species, including mammals, birds, reptiles, and fish. Moreover, the mutated proline at this position is highly conserved in the large majority of the Ig-like domains of not only human filamins A, B, and C, but even in filamins from *Drosophila melanogaster* and *Dictyostelium discoideum*. As the level of FLNC is not reduced in patient muscle, the expression from both mutant alleles is apparently not impaired; however, the mutant protein is less stable. Our combined biochemical findings suggest that the reduced stability of the mutant protein might be compensated by forced expression or translation of the respective transcripts. The concept of misfolded FLNC impinging on disintegration of sarcomeric structures and concomitant aggregate formation is supported by our immunofluorescence finding showing sarcoplasmic protein aggregates immunoreactive for FLNC and known marker proteins including Xin and XIRP2, as well as our electron microscopic findings revealing electron-dense inclusions reminiscent of myofibrillar rods and probably represent advanced sarcomeric lesions along with degenerated myofibrils and other sarcoplasmic components. It was postulated that the lesion pathology and not the formation of protein aggregates may be the major contributing factor to muscle weakness in patients (Chevessier et al., 2015). However, one might assume that both, the presence of lesions and the concomitant occurrence of protein aggregates impinge on general proteostasis of the muscle cells and thus lead to further pathological cascades significantly contributing to muscle cell vulnerability. Given that in our case the biopsy was taken at 30 months of age, well after the occurrence of the first symptoms at birth, the biopsy represents a stage of progressed disease rather than an early stage. This is confirmed by the results of our histological and enzyme histochemistry studies. Moreover, the results of our proteomic profiling revealed affection of proteins involved in a diversity of cellular processes, such as sugar metabolism and signaling cascades, thus supporting the concept that lesions and aggregate-build-up secondarily affect processes beyond cytoskeleton and protein clearance. This is in accordance with the notion that FLNC is a highly dynamic protein involved in signaling pathway control and metabolic regulation (Furst et al., 2013; Leber et al., 2016; Molt et al., 2014). Verification of our proteomic findings revealing increased abundance of transketolase in muscle fibers of our patient further accords with this assumption. Given that a variety of myosin- or myosin-modulating proteins are known to be predominantly expressed in certain fiber types, a vulnerability of those—as identified by our proteomic profiling—most likely suggests a predominance of type 1 fibers (a finding observed in a variety of congenital myopathies). Increased expression of galectin-3 as a known promoter of myogenesis improving skeletal muscle function in *mdx* mice (mouse model of Duchenne muscular dystrophy; DMD; Rancourt et al., 2018) suggests activation of myocellular compensatory mechanisms. However, the progressive nature of the muscle disease in our patient with current loss of ambulation, might accord with the assumption that the pathological cascades triggered by the lesions and concomitant protein aggregate formation not only significantly contributed to muscle cell vulnerability but also led to apoptosis.

Previous proteomic studies of protein aggregates in dominant filaminopathy cases allowed the identification of potential marker proteins (Kley, Maerkens, et al., 2013). To further address the pathogenicity of this first recessive *FLNC* variant, the expression and localization of several of these markers were investigated in our patient. Indeed, most of these marker proteins were also found in the protein aggregates in the muscle fibers of our patient. This not only supports the pathogenicity of the homozygous c.1325C>G (p.Pro442Arg) *FLNC* mutation, but also suitability of these proteins as markers for protein aggregation in filaminopathy. Further evidence for pathogenicity is provided by the results of our ultrastructural investigations focusing on pathomorphological findings characteristic for filaminopathies and revealing pathological findings indicative for an MFM-filaminopathy.

Interestingly, heart tissue derived from an individual with *FLNC*-truncating variant showed reduced levels of the FLNC compared to control samples by Western blot analysis (Begay et al., 2016). In addition, is has been demonstrated that a reduction in *flncb* (ortholog of human FLNC) RNA expression in zebrafish results in structural and functional cardiac abnormalities (Begay et al., 2016), further supporting the theory that reduced FLNC expression may be causative for cardiac dysfunctions (Begay et al., 2018). Given that in our case the level of FLNC is not reduced, one might assume that this molecular finding correlates with the lack of cardiac involvement in our case.

Although both parents are heterozygous for the mutation, both are "classified" as clinically healthy (neither signs of a neuromuscular nor cardiac disease) after multiple clinical examinations including cardiac screening. In this context, it is also important to note that three preceding generations did not show the presence of a muscle or cardiac disorder. Hence, a dominant effect of the c.1325C>G; p.Pro442Arg *FLNC* mutation seems to be unlikely and by the same token indicates this amino acid substitution to be the first recessive mutation described for FLNC thus far. However, the contribution of another mutation (for instance in a gene not yet linked to the manifestation of a neuromuscular disease) cannot be excluded. Given that *FLNC* mutations published so far are very frequently associated with the manifestation of cardiac symptoms, we recommended an annual cardiac examination of the index patient to exclude development of cardiomyopathy, and regular neuromuscular and cardiac examination of the parents.

The notion that homozygous mutant protein expression may severely aggravate the disease phenotype is corroborated by recent findings in a mouse model of the human p.W2710X filaminopathy mutation. While heterozygous expression of the mutant protein results in a relatively mild phenotype (Chevessier et al., 2015).

5 | CONCLUSIONS

Hence, our combined findings confirm the pathogenicity of the c.1325C>G/p.Pro442Arg *FLNC*/FLNC variant in the rod domain of FLNC as the first homozygous mutation of filaminopathies presumably associated with a recessive mode of inheritance. In contrast to muscular disease caused by heterozygous *FLNC* mutations, here the disease course started neonatally as a congenital proximal myopathy developing into a distal form in childhood. Our histological, biochemical, and ultrastructural examinations revealed typical signs of an MFM that is compatible to the expression of high levels of a misfolded, toxic variant of FLNC. The unique homozygous *FLNC* mutation in our patient results in a congenital presentation of the disease with a very progressive development. Thus, our combined data significantly extend the currently recognized clinical and genetic spectrum of filaminopathies.

ACKNOWLEDGMENTS

We thank Hannelore Mader, Claudia Krude, Ronja Kardinal, Karin Bois, Lisa Wadephul, Swantje Hertel, and Nancy Meyer for their expert technical assistance. A. R. acknowledges the support from the AFM (Grant 21644). A. R., U. S., and A. S. also acknowledge funding in the framework of the NME-GPS project by the European Regional Development Fund (ERDF). Moreover, L. K. and A. S. acknowledge the support by the Ministerium für Kultur und Wissenschaft des Landes Nordrhein-Westfalen, the Regierende Bürgermeister von Berlin—inkl. Wissenschaft und Forschung, and the Bundesministerium für Bildung und Forschung. This study was supported by the German Research Foundation (Multilocation DFG-Research Units FOR1352 and FOR2743, D.O.F.); MYO-SEQ was funded by Sanofi Genzyme, Ultragenyx, LGMD2I Research Fund, Samantha J Brazzo Foundation, LGMD2D Foundation and Kurt+Peter Foundation, Muscular Dystrophy UK, and Coalition to Cure Calpain-3. Through the Wiley/Projekt DEAL agreement in Germany, we are eligible for open access funding: account code D709, institution: Universitätsklinikum Essen.

CONFLICT OF INTERESTS

The authors declare that there are no conflict of interests.

DATA AVAILABILITY STATEMENT

The mass spectrometry proteomics data have been deposited to the ProteomeXchange Consortium via the PRIDE (Perez-Riverol et al., 2019) partner repository with the data set identifier PXD016657.

ORCID

Heike Kölbel http://orcid.org/0000-0001-9629-7053
Peter F. M. van der Ven http://orcid.org/0000-0002-9750-8913

REFERENCES

Ader, F., De Groote, P., Reant, P., Rooryck-Thambo, C., Dupin-Deguine, D., Rambaud, C., … Richard, P. (2019). FLNC pathogenic variants in patients with cardiomyopathies: Prevalence and genotype–phenotype correlations. *Clinical Genetics*, *96*(4), 317–329. https://doi.org/10.1111/cge.13594

Begay, R. L., Graw, S. L., Sinagra, G., Asimaki, A., Rowland, T. J., Slavov, D. B., … Taylor, M. R. G. (2018). Filamin C truncation mutations are associated with arrhythmogenic dilated cardiomyopathy and changes in the cell–cell adhesion structures. *JACC: Clinical Electrophysiology*, *4*(4), 504–514. https://doi.org/10.1016/j.jacep.2017.12.003

Begay, R. L., Tharp, C. A., Martin, A., Graw, S. L., Sinagra, G., Miani, D., … Taylor, M. R. (2016). FLNC gene splice mutations cause dilated cardiomyopathy. *JACC: Basic to Translational Science*, *1*(5), 344–359. https://doi.org/10.1016/j.jacbts.2016.05.004

Bhardwaj, G., Dorr, M., Sappa, P. K., Ameling, S., Dhople, V., Steil, L., … Hammer, E. (2017). Endomyocardial proteomic signature corresponding to the response of patients with dilated cardiomyopathy to immunoadsorption therapy. *Journal of Proteomics*, *150*, 121–129. https://doi.org/10.1016/j.jprot.2016.09.001

Chevessier, F., Schuld, J., Orfanos, Z., Plank, A. C., Wolf, L., Maerkens, A., … Schroder, R. (2015). Myofibrillar instability exacerbated by acute exercise in filaminopathy. *Human Molecular Genetics*, *24*(25), 7207–7220. https://doi.org/10.1093/hmg/ddv421

Claeys, K. G., van der Ven, P. F., Behin, A., Stojkovic, T., Eymard, B., Dubourg, O., … Furst, D. O. (2009). Differential involvement of sarcomeric proteins in myofibrillar myopathies: A morphological and immunohistochemical study. *Acta Neuropathologica*, *117*(3), 293–307. https://doi.org/10.1007/s00401-008-0479-7

Duff, R. M., Tay, V., Hackman, P., Ravenscroft, G., McLean, C., Kennedy, P., … Laing, N. G. (2011). Mutations in the N-terminal actin-binding domain of filamin C cause a distal myopathy. *American Journal of Human Genetics*, *88*(6), 729–740. https://doi.org/10.1016/j.ajhg.2011.04.021

Fukushima, A., Kinugawa, S., Takada, S., Matsushima, S., Sobirin, M. A., Ono, T., … Tsutsui, H. (2014). (Pro)renin receptor in skeletal muscle is involved in the development of insulin resistance associated with postinfarct heart failure in mice. *American Journal of Physiology, Endocrinology and Metabolism*, *307*(6), E503–E514. https://doi.org/10.1152/ajpendo.00449.2013

Furst, D. O., Goldfarb, L. G., Kley, R. A., Vorgerd, M., Olive, M., & van der Ven, P. F. (2013). Filamin C-related myopathies: Pathology and mechanisms. *Acta Neuropathologica*, *125*(1), 33–46. https://doi.org/10.1007/s00401-012-1054-9

Guergueltcheva, V., Peeters, K., Baets, J., Ceuterick-de Groote, C., Martin, J. J., Suls, A., … Jordanova, A. (2011). Distal myopathy with upper limb predominance caused by filamin C haploinsufficiency. *Neurology*, *77*(24), 2105–2114. https://doi.org/10.1212/WNL.0b013e31823dc51e

Gueugneau, M., d'Hose, D., Barbe, C., de Barsy, M., Lause, P., Maiter, D., … Thissen, J. P. (2018). Increased Serpina3n release into circulation during glucocorticoid-mediated muscle atrophy. *Journal of Cachexia, Sarcopenia and Muscle*, *9*(5), 929–946. https://doi.org/10.1002/jcsm.12315

Katona, I., Weis, J., & Hanisch, F. (2014). Glycogenosome accumulation in the arrector pili muscle in Pompe disease. *Orphanet Journal of Rare Diseases*, *9*, 17. https://doi.org/10.1186/1750-1172-9-17

Kley, R. A., Maerkens, A., Leber, Y., Theis, V., Schreiner, A., van der Ven, P. F., … Marcus, K. (2013). A combined laser microdissection and mass spectrometry approach reveals new disease relevant proteins accumulating in aggregates of filaminopathy patients. *Molecular & Cellular Proteomics*, *12*(1), 215–227. https://doi.org/10.1074/mcp.M112.023176

Kley, R. A., van der Ven, P. F., Olive, M., Hohfeld, J., Goldfarb, L. G., Furst, D. O., & Vorgerd, M. (2013). Impairment of protein degradation in myofibrillar myopathy caused by FLNC/filamin C mutations. *Autophagy*, *9*(3), 422–423. https://doi.org/10.4161/auto.22921

Kolbel, H., Hathazi, D., Jennings, M., Horvath, R., Roos, A., & Schara, U. (2019). Identification of candidate protein markers in skeletal muscle

of laminin-211-deficient CMD type 1A-patients. *Frontiers in Neurology*, *10*, 470. https://doi.org/10.3389/fneur.2019.00470

Leber, Y., Ruparelia, A. A., Kirfel, G., van der Ven, P. F., Hoffmann, B., Merkel, R., … Furst, D. O. (2016). Filamin C is a highly dynamic protein associated with fast repair of myofibrillar microdamage. *Human Molecular Genetics*, *25*(13), 2776–2788. https://doi.org/10.1093/hmg/ddw135

Lindqvist, J., Torvaldson, E., Gullmets, J., Karvonen, H., Nagy, A., Taimen, P., & Eriksson, J. E. (2017). Nestin contributes to skeletal muscle homeostasis and regeneration. *Journal of Cell Science*, *130*(17), 2833–2842. https://doi.org/10.1242/jcs.202226

Lukjanenko, L., Jung, M. J., Hegde, N., Perruisseau-Carrier, C., Migliavacca, E., Rozo, M., … Bentzinger, C. F. (2016). Loss of fibronectin from the aged stem cell niche affects the regenerative capacity of skeletal muscle in mice. *Nature Medicine*, *22*(8), 897–905. https://doi.org/10.1038/nm.4126

Molt, S., Buhrdel, J. B., Yakovlev, S., Schein, P., Orfanos, Z., Kirfel, G., … Furst, D. O. (2014). Aciculin interacts with filamin C and Xin and is essential for myofibril assembly, remodeling and maintenance. *Journal of Cell Science*, *127*(Pt 16), 3578–3592. https://doi.org/10.1242/jcs.152157

Nolte, H., MacVicar, T. D., Tellkamp, F., & Krüger, M. (2018). Instant clue: A software suite for interactive data visualization and analysis. *Scientific Reports*, *8*(1), 12648. https://doi.org/10.1038/s41598-018-31154-6

Pasternack, G. R., & Racusen, R. H. (1989). Erythrocyte protein 4.1 binds and regulates myosin. *Proceedings of the National Academy of Sciences of the United States of America*, *86*(24), 9712–9716. https://doi.org/10.1073/pnas.86.24.9712

Perez-Riverol, Y., Csordas, A., Bai, J., Bernal-Llinares, M., Hewapathirana, S., Kundu, D. J., … Vizcaíno, J. A. (2019). The PRIDE database and related tools and resources in 2019: Improving support for quantification data. *Nucleic Acids Research*, *47*(D1), D442–D450. https://doi.org/10.1093/nar/gky1106

Rancourt, A., Dufresne, S. S., St-Pierre, G., Levesque, J. C., Nakamura, H., Kikuchi, Y., … Sato, S. (2018). Galectin-3 and *N*-acetylglucosamine promote myogenesis and improve skeletal muscle function in the mdx model of Duchenne muscular dystrophy. *FASEB Journal*, *32*(12), 6445–6455. https://doi.org/10.1096/fj.201701151RRR

Roos, A., Buchkremer, S., Kollipara, L., Labisch, T., Gatz, C., Zitzelsberger, M., … Weis, J. (2014). Myopathy in Marinesco-Sjogren syndrome links endoplasmic reticulum chaperone dysfunction to nuclear envelope pathology. *Acta Neuropathologica*, *127*(5), 761–777. https://doi.org/10.1007/s00401-013-1224-4

Roos, A., Thompson, R., Horvath, R., Lochmuller, H., & Sickmann, A. (2018). Intersection of proteomics and genomics to "solve the unsolved" in rare disorders such as neurodegenerative and neuromuscular diseases. *Proteomics: Clinical Applications*, *12*(2), 1–6. https://doi.org/10.1002/prca.201700073

Rossi, D., Palmio, J., Evila, A., Galli, L., Barone, V., Caldwell, T. A., … Sorrentino, V. (2017). A novel FLNC frameshift and an OBSCN variant in a family with distal muscular dystrophy. *PLOS One*, *12*(10), e0186642. https://doi.org/10.1371/journal.pone.0186642

Selcen, D. (2011). Myofibrillar myopathies. *Neuromuscular Disorders*, *21*(3), 161–171. https://doi.org/10.1016/j.nmd.2010.12.007

Shatunov, A., Olive, M., Odgerel, Z., Stadelmann-Nessler, C., Irlbacher, K., van Landeghem, F., … Goldfarb, L. G. (2009). In-frame deletion in the seventh immunoglobulin-like repeat of filamin C in a family with myofibrillar myopathy. *European Journal of Human Genetics*, *17*(5), 656–663. https://doi.org/10.1038/ejhg.2008.226

Töpf, A., Johnson, K., Bates, A., Phillips, L., Chao, K. R., England, E. M., … Straub, V. (2020). Sequential targeted exome sequencing of 1001 patients affected by unexplained limb-girdle weakness. *Genetics in Medicine*. https://doi.org/10.1038/s41436-020-0840-3

Valdes-Mas, R., Gutierrez-Fernandez, A., Gomez, J., Coto, E., Astudillo, A., Puente, D. A., … Lopez-Otin, C. (2014). Mutations in filamin C cause a new form of familial hypertrophic cardiomyopathy. *Nature Communications*, *5*, 5326. https://doi.org/10.1038/ncomms6326

van der Flier, A., & Sonnenberg, A. (2001). Structural and functional aspects of filamins. *Biochimica et Biophysica Acta/General Subjects*, *1538*(2–3), 99–117.

Vorgerd, M., van der Ven, P. F., Bruchertseifer, V., Lowe, T., Kley, R. A., Schroder, R., … Huebner, A. (2005). A mutation in the dimerization domain of filamin c causes a novel type of autosomal dominant myofibrillar myopathy. *American Journal of Human Genetics*, *77*(2), 297–304. https://doi.org/10.1086/431959

Wang, S., Liu, J., Wu, D. I., Pang, X., Zhao, J., & Zhang, X. (2015). Pro-inflammatory effect of fibrinogen on vascular smooth muscle cells by regulating the expression of PPARalpha, PPARgamma and MMP-9. *Biomedical Reports*, *3*(4), 513–518. https://doi.org/10.3892/br.2015.459

Zhang, C., Wang, C., Li, Y., Miwa, T., Liu, C., Cui, W., … Du, J. (2017). Complement C3a signaling facilitates skeletal muscle regeneration by regulating monocyte function and trafficking. *Nature Communications*, *8*(1), 2078. https://doi.org/10.1038/s41467-017-01526-z

SUPPORTING INFORMATION

Additional supporting information may be found online in the Supporting Information section.

How to cite this article: Kölbel H, Roos A, van der Ven PFM, et al. First clinical and myopathological description of a myofibrillar myopathy with congenital onset and homozygous mutation in *FLNC*. *Human Mutation*. 2020;41:1600–1614. https://doi.org/10.1002/humu.24062